Mechanistic Studies of the Acidolysis Reactions Occurring in Silicon-Containing Bilayer Photoresists

Ilya Zharov† and Josef Michl*

Department of Chemistry and Biochemistry, University of Colorado, Boulder, Colorado 80309-0215

Mark H. Sherwood, Ratnam Sooriyakamaran, C. E. Larson, Richard A. DiPietro, Gregory Breyta, and Gregory M. Wallraff*

IBM Almaden Research Center, 650 Harry Road K95/801, San Jose, California 95120-6099

Received July 2, 2001. Revised Manuscript Received October 31, 2001

As the feature sizes of semiconductor devices continue to shrink, there is an increasing interest in thin film imaging approaches such as silicon-based bilayer resists. We have developed such a resist based on a copolymer of 4-hydroxystyrene with a silicon-containing monomer, which functions simultaneously as the acid-sensitive component and a source of O_2 etch resistance. In an attempt to understand the reactions that occur in the photoresist film, the acidolysis reactions of the 2-[tris(trimethylsilyl)silyl]ethyl moiety have been studied in solution. Acid-catalyzed cleavage of the model 2-trimethylsilylethyl acetate in solution proceeds via a nucleophilic attack on the silicon atom of the protonated acetate. Protonation of 2-[tris(trimethylsilyl)silyl]ethyl acetate is postulated to lead to a bridged siliconium cation, which reacts with nucleophiles along three pathways and yields products in which a nucleophile is attached to a silicon atom. This mechanism is consistent with the silylation of phenolic hydroxyl groups in the photoresist film consisting of a copolymer of 4-hydroxystyrene with 2-[tris(trimethylsilyl)silyl]ethyl methacrylate, observed during photolithographic processing.

Introduction

Thin film imaging (TFI) that employs bilayer photoresists[1] has long been proposed as a candidate in the technology for high-resolution lithography. In this approach, an image is generated in a silicon-containing thin film and then transferred to a thicker polymeric underlayer in an oxygen reactive ion etch (O_2-RIE) step. The potential advantages of this procedure include better resolution at a given depth of focus (DOF), improved ability to print high aspect ratios (height/width) at small feature sizes, and minimization of resist−substrate interactions including reflective notching caused by topography, resist "footing", and standing wave formation.[2] The process flow for a bilayer resist system is shown in Figure 1 along with representative resist profiles for both the initial imaged resist pattern and the final profile after O_2-RIE.

To date, the continued improvement in single-layer resist performance has met the current manufacturing requirements and more complex TFI approaches such as bilayer resists have not been required. However, as

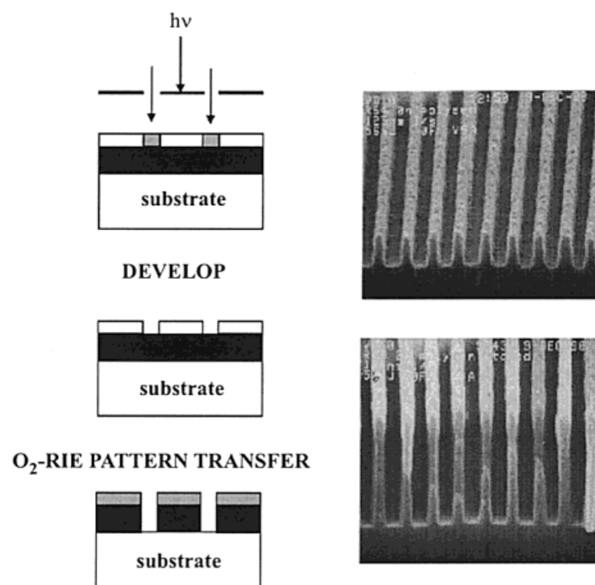

Figure 1. Left, schematic representation of the three-step bilayer resist development process. Top right, 125 nm line/space array printed in an optimized photoresist formulation based on the 2-[tris(trimethylsilyl)silyl]ethyl methacrylate monomer. Bottom right, photoresist image following oxygen reactive ion etch pattern transfer.

the semiconductor industry strives to print ever smaller features at a given wavelength (with 248 nm imaging now being used to print 130 nm features) and as new fabrication techniques are implemented, alternative

* To whom correspondence should be addressed.

† Present address: Beckman Institute for Advanced Science and Technology, University of Illinois at Urbana-Champaign, 405 North Mathews Ave., Urbana, IL 61801.

(1) Miller, R. D.; Wallraff, G. M. In *Adv. Mater. Opt. Electron.* **1994**, *4*, 95.

(2) Willson, C. G. In *Introduction to Microlithography,* 2nd ed.; ACS Professional Reference Book, American Chemical Society: Washington, DC, 1994; Chapter 2.

10.1021/cm010660i CCC: $22.00 © 2002 American Chemical Society
Published on Web 01/26/2002

Scheme 1

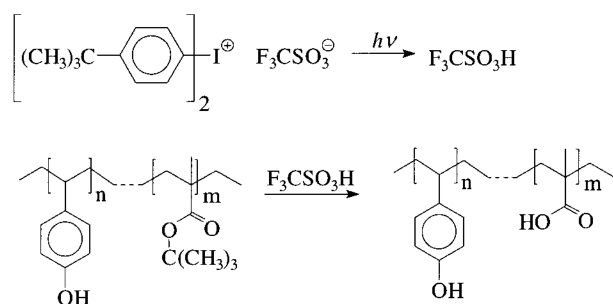

resist processes are receiving greater consideration. In the future, as optical lithography moves to shorter wavelengths (193 and 157 nm) and even the very short wavelengths (10−13 nm) of "extreme" UV,[3] issues with resist transparency and DOF will become critical and TFI approaches will become even more attractive.

A number of different strategies have been employed in the design of silicon-based bilayer resists over the past several years,[1] with the goal of incorporating enough silicon to provide adequate O_2-RIE etch resistance. While the silicon content required for good etch selectivity is dependent on the specifics of the etch process, prior studies have shown that a good practical target is a value of at least 10 wt %.[4] As the resolution requirements for chemically amplified resists continue to shrink, achieving this high level of silicon content in a high-resolution high-contrast resist poses a considerable challenge.

Scheme 1 shows the reactions that occur in a typical chemically amplified resist.[5] In this example, the resist consists of a copolymer of 4-hydroxystyrene with another monomer containing an acid-labile pendent group, *t*-butyl methacrylate, and an onium salt photoacid generator (PAG). Upon resist exposure, a low concentration of a strong Brønsted acid (triflic acid in the illustrated case) is photochemically generated. Subsequent thermolysis of the polymer, mediated by the acid catalyst, fragments the pendent *t*-butyl ester groups. In this fashion, the phenolic copolymer, whose composition has been optimized to make it essentially insoluble in 0.26 N tetra-*n*-butylammonium hydroxide (the industry standard photoresist developer) is converted into a more acidic phenol−carboxylic acid copolymer that dissolves cleanly in the exposed regions. There are other systems that can be made to function in this fashion, and a variety of different monomers and protecting groups have been developed for use in 248 and 193 nm single layer resists. In addition to the photoresponse and dissolution properties described above, properties such as etch resistance, adhesion, transparency, and thermal behavior all need to be optimized. As a consequence, the incorporation of a high concentration of an inert silicon monomer is likely to complicate resist design even further as it impacts the other resist properties. For this reason, it may prove advantageous to use a silicon-based monomer that is itself acid labile since its dual function can simplify the resist design. The properties of such a monomer and its copolymers are the subject of this report.

Chart 1

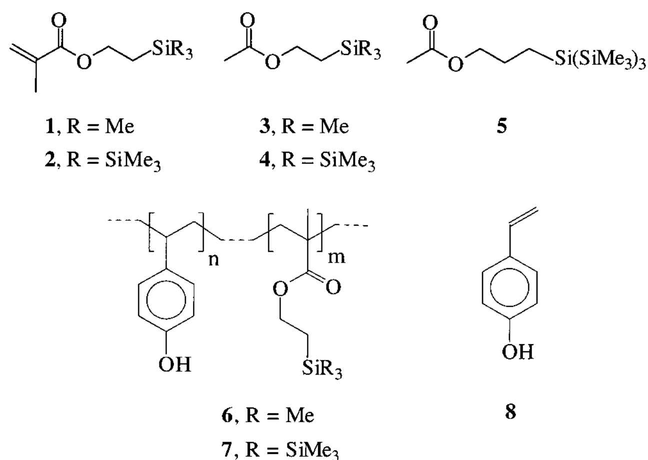

Results

The monomers, 2-(trimethylsilyl)ethyl methacrylate (**1**) and 2-[tris(trimethylsilyl)silyl]ethyl methacrylate (**2**), and the model compounds, 2-(trimethylsilyl)ethyl acetate (**3**), 2-[tris(trimethylsilyl)silyl]ethyl acetate (**4**), and 3-[tris(trimethylsilyl)silyl]propyl acetate (**5**), are shown in Chart 1. Copolymers **6** and **7** were synthesized by a copolymerization of **1** and **2**, respectively, with 4-hydroxystyrene (**8**). Copolymers **6** and **7** typically had glass transition temperatures of approximately 160 °C (154 °C for the 80:20 copolymer **7**) and showed no evidence of thermal decomposition or weight loss at temperatures below 220 °C.

These copolymers function in a fashion analogous to that shown in Figure 1. The copolymerized methacrylate reacts with the photogenerated acid to produce copolymerized methacrylic acid, which increases the solubility of the resist film in the areas exposed to light. In this fashion, the monomers **1** and **2** function both as a source of silicon and as an acid-labile "polarity switch" which renders the exposed areas of the film soluble in basic developers. If the 3-silylated propyloxy ester **5** is employed instead of the 2-silylated ethoxy linker esters **3** or **4**, the system is inert to acid-catalyzed cleavage. The reason behind this is described below.

Copolymers **6** and **7** can be used as positive resists over a fairly wide composition range (copolymer ratios of **8** to **1** or **2** of 75:25−90:10). The photospeed and resist contrast are comparable to the analogous *t*-butyl methacrylate-based systems shown in Scheme 1. Figure 2 shows some preliminary results obtained on the 80:20/bis(*t*-butylphenyl)iodonium triflate resist system **7** exposed on a Nikon DUV stepper (NA of 0.42).[6]

The lithographic performance of the copolymer resists **6** and **7** can be further optimized through incorporation of other monomers and resist additives. High-performance resists based on this chemistry can be used in a variety of applications. Figure 3 shows an electron

(3) Hawryluk, A. M.; Seppala, L. G. *J. Vac. Sci. Technol., B* **1988**, *6*, 2162.
(4) Hayashi, N.; Ueno, T.; Shiraishi, H.; Nidhida, T.; Toriumi, M.; Nonogaki, S. *ACS Symp. Ser.* **1987**, *346*, 211.
(5) (a) MacDonald, S.; Willson, C. G.; Frechet, J. M. J. *Acc. Chem. Res.* **1994**, *27*, 15. (b) Ito, H. *SPIE Adv. Resist Technol. Lithogr.* **1999**, *2*, 3678.
(6) Sooriyakumaran, R.; Wallraff. G. M.; Larson, C. E.; Fenzel-Alexander, D.; DiPietro, R.; Hofer, R. D.; Opitz, J.; LaTulip, D.; Simons J.; Petrillo, K.; Babich, K.; Angelopoulos, M.; Lin G.; Katnani, A. *SPIE Adv. Resist Technol. Lithogr.* **1998**, *3333*, 219.

Scheme 2

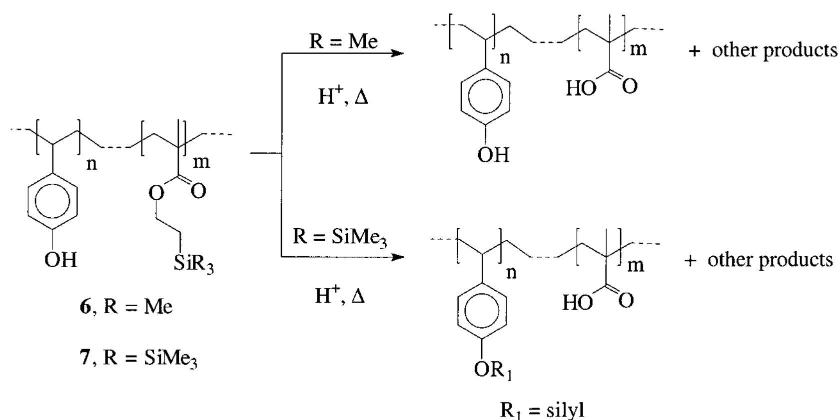

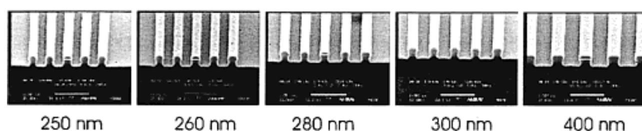

Figure 2. Line/space arrays of varying feature size printed at a 18 mJ/cm^2 single dose in the 2-[tris(trimethylsilyl)silyl]-ethyl methacrylate 80:20/di-*t*-butylphenyliodonium triflate resist (Nikon 248 nm exposure system, NA 0.42, binary mask), with a 1 μm size bar.

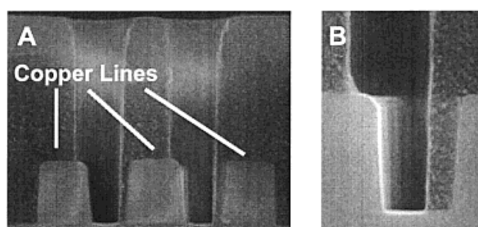

Figure 3. Bilayer resist images following development, O_2-RIE and SiO_2 pattern transfer etch steps: A, SEM of etched pattern over underlying copper topography and B, Magnified view.

micrograph of a device structure where a bilayer resist can be especially advantageous. In this example, the resolution requirements are relatively modest at 250 nm; however, reflections from the underlying metal structures make printing features such as this very difficult using a single-layer resist.

On exposure, the films shrink by ~12% due to the volatilization of reaction products. NMR analysis of a resist film based on the 70:30 copolymer **6** following exposure and postbake showed a single silicon species: hexamethyldisiloxane. ^{29}Si NMR analysis of a resist film based on the 80:20 copolymer **7** following exposure and postbake showed the presence of many silicon-containing species. The corresponding ^{13}C NMR spectrum provided evidence for significant amounts (18%) of silylated phenolic hydroxyl groups, with new resonances due to the polymer-bound species appearing at 120.2 ppm. IR analysis of processed films of the 80:20 resist **7** is consistent with the formation of the Si−O functionality. The plot in Figure 4 shows the growth of the Si−O absorption mirroring the disappearance of an absorption band assigned to the tris(trimethylsilyl) group as a function of the imaging dose.

Due to the complexities in identifying the reaction products that are produced in the resist films (Scheme 2) we turned to solution experiments on model com-

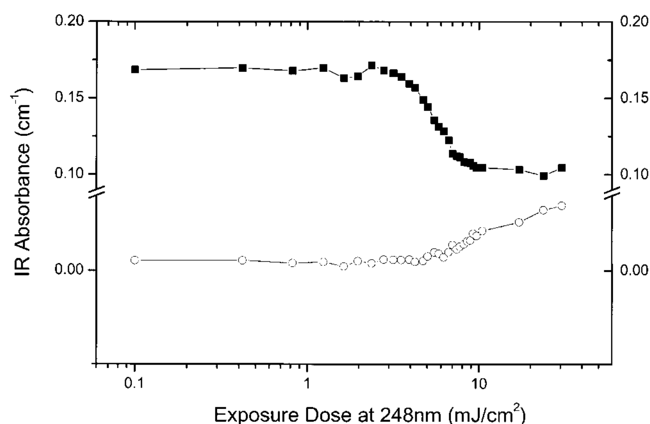

Figure 4. IR absorbances due to the silyl protecting group (838 cm^{-1}, closed squares) and siloxane formation (1053 cm^{-1}, open circles) as a function of exposure dose in an 2-[tris-(trimethylsilyl)silyl]ethyl methacrylate 80:20/bis(*t*-butylphenyl)iodonium triflate resist film.

Scheme 3

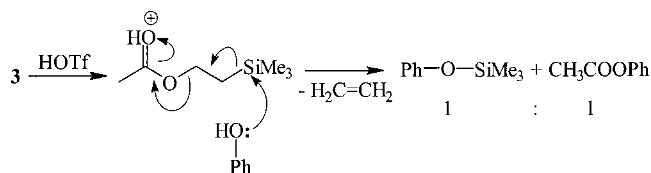

pounds to try and help in the elucidation of the reactions of the copolymer **7**. Model compounds **3**, **4**, and **5** were studied. Compounds **3** and **4** are analogous to the structures produced when monomers **1** and **2**, respectively, are incorporated into the copolymers **6** or **7**, and the model compound **5** with a γ-silyl group was studied for comparison.

When **3** was treated with HOTf in wet chloroform, the only silicon-containing product was hexamethyldisiloxane. Ethylene and acetic acid were also produced. In dry phenol, the same reaction produced trimethylphenoxysilane, phenyl acetate, and ethylene (Scheme 3).

Products of the reaction of **4** with HOTf in dry phenol are shown in Scheme 4, and the products of a similar reaction in dry methanol are presented in Scheme 5.

While **5** was unreactive, the reaction of **4** with HOTf in dry chloroform resulted in several products. Unfortunately, they were not stable under preparative GC conditions, and we were unable to separate and isolate

Scheme 4

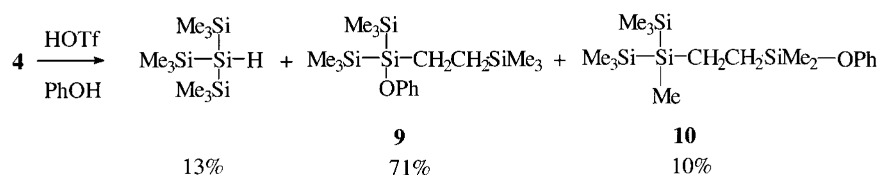

Scheme 5

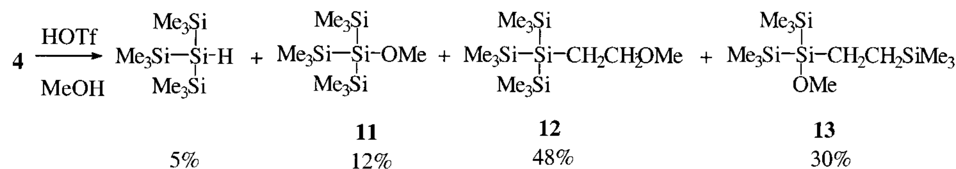

them. However, from the NMR and MS data it was evident that in this case, acetate acted as a nucleophile, and products similar to those observed in the case of acidic cleavage of **4** in phenol and methanol were formed. In particular, judging by NMR spectra, bis(trimethylsilyl)[2-(trimethylsilyl)ethyl]acetoxysilane, analogous to **9** and **13**, constituted about half of the resulting mixture.

We measured the first-order rate constant of acid-catalyzed cleavage of **4** in $CD_3OD/CDCl_3$ (60:40 mixture) at 25 °C to be 2.9×10^{-5} s^{-1}. Under the same conditions, the rate constant for *t*-butyl acetate was 1.4×10^{-5} s^{-1}.

Discussion

We believe that the reactions of the model compounds **3** and **4** reflect the well-recognized ability of the β-silyl substituent to stabilize carbocations of the type $R_3SiCH_2CH_2^+$.[7] This stabilization is believed to be due to both the electropositive nature of silicon and hyperconjugation involving donation of the C–Si σ electrons into the empty p orbital of the carbocation.[7] β-Silylated carbocations are significantly more stable than unsubstituted carbocations, with stabilization energies similar to that of a *t*-butyl cation.[8] These reactive intermediates are unstable in condensed media, and only recently, has one such cation been characterized spectroscopically in solution.[9] Their fragmentation occurs with transfer of the silicon substituent to a nucleophile. In the case of simple β-silylated carbocations, this is believed to occur via nucleophilic attack at silicon followed by a loss of tetravalent silicon.[9] Bulky substituents on the silicon may modify this reactivity.

One would expect the following mechanism for the acidolysis reactions of **3** and **4** (Schemes 3 and 6). The first step probably involves a fast proton transfer equilibrium between triflic acid and the ester group of **3** and **4** (and similarly, of **6** or **7**). Step two is the slow, rate-determining cleavage to generate free carboxylic acid and a β-silylated carbocation, consistent with specific acid catalysis of the type described previously.[10] The facile formation of this cation is the result of the β-silyl stabilizing effect,[7] which is supported by the fact that acidolysis of **5**, the acetate of a γ-silylated alcohol, shows no reaction with triflic acid in methanol and phenol. The fate of the liberated cation depends on the nature of the group R. Rapid nucleophilic attack at silicon and a loss of the silyl group are likely to occur unless the substituents on silicon are bulky or electron withdrawing.[9] In the case of bulky $SiMe_3$ substituents, fragmentation and rearrangements would accompany the reaction with nucleophiles present in the reaction mixture.

Scheme 6

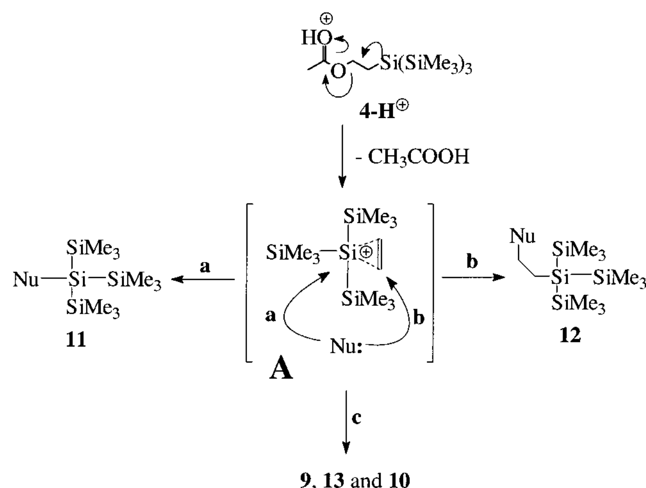

Reactions observed for the model compounds are in line with these expectations. The reaction of **3** (Scheme 3) appears to occur via a nucleophilic attack at the silicon atom of the protonated acetate, followed by the loss of ethylene and formation of phenoxy- or hydroxytrimethylsilane. The latter is known[11] to dimerize under acidic conditions to give hexamethyldisiloxane. The reaction of **4** (Scheme 6) fits the same pattern: rapid protonation followed by a slower cleavage, which yields acetic acid and the 2-tris(trimethylsilyl)silyl substituted carbocation. The fact that the acidolysis rate for **4** is somewhat higher than that for *t*-butyl acetate is attributed to the β-silyl stabilization effect, which makes the resulting carbocation about as stable as the *t*-butyl cation, formed in the case of *t*-butyl acetate. A bridged structure for the β-tris(trimethylsilyl) substituted carbocation (**A** in Scheme 6) is the most economical

(7) Siehl, H.-U.; Müller, T. In *The Chemistry of Organic Silicon Compounds*; Rappoport, Z., Apeloig, Y., Eds.; John Wiley & Sons Ltd.: New York, 1998; p 595.
(8) Shin, S.; Beauchamp, J. *J. Am. Chem. Soc.* **1989**, *111*, 900.
(9) Lambert, J. B.; Zhao, Y. *J. Am. Chem. Soc.* **1996**, *118*, 7867.
(10) Wallraff, G. M.; Hinsberg, W.; Houle, F.; Opitz, J.; Hopper, D.; Hutchinson, J. *Proc. SPIE-Int. Soc. Opt. Eng.* **1995**, *2438*, 182.
(11) Brook, M. A. *Silicon in Organic, Organometallic, and Polymer Chemistry*; John Wiley: New York, 2000.

postulate that accounts for the formation of mixtures of products with the nucleophile attached to either a carbon or a silicon atom in all cases studied.

Formation of bridged siliconium cations is precedented.[7] For example, a stable silanorbornyl cation[12] is an almost symmetrical bridged β-silylated carbocation with siliconium cation character. The open β-silylethyl cation $H_3Si-CH_2-CH_2^+$ is calculated not to be a potential energy minimum at high levels of theory; it collapses to the bridged silylethyl cation which is best described as a π-complex between a silylium ion and ethylene.[13] Calculations suggest that in the reaction of H_3Si^+ and ethylene, both the ethylsilylium ion and bridged silylethyl cations are formed.[13] Calculations also showed that in $H_3Si-CH_2-CH^+-CH_3$, the silyl group is significantly bent toward the positively charged carbon atom.[14] Several studies in the gas phase pointed to the formation of both bridged and open ions in the case of $C_5H_{13}Si^+$.[15] In a gas-phase study of substituted styrenes, it was concluded that a partially bridged structure is favorable for $Ar-CH^+-CH_2-SiMe_3$.[16] Several solvolytic studies suggested the formation of bridged cations in the cases of *erythro*-$Me_3Si-CHBr-CHBrMe$ (based on the structures of solvolysis products)[17] and of various $Me_3Si-CH_2-CH_2-Hal$ derivatives (based on secondary deuterium isotope effects[18,19] and on the conformational dependence of the reaction rates[20]). A partially bridged structure was suggested for an intermediate in the solvolysis of $Ar-CH(X)-CH_2-SiMe_3$.[17] The formation of a bridged cation was also consistent with observations made in the solvolysis study of $Me_3Si-CH(Ph)-CH_2-Cl$.[20]

We propose that the presently postulated bridged cation **A** reacts with nucleophiles along three pathways (Scheme 6). In pathway **a**, the nucleophile attacks the positively charged silicon atom, providing the product **11** and ethylene. This pathway is followed only for methanol, while with phenol, the corresponding product is not observed. The formation of tris(trimethylsilyl)silane,[21] which occurs to a small degree in both phenol and methanol, can be formally attributed to the pathway **a** as well. The source of the hydride anion is not obvious; it could be methanol itself, and phenol could act both as an electron and a hydrogen atom donor.

In pathway **b**, the nucleophile attacks one of the bridging carbon atoms, leading to a product analogous to that expected from an open-chain β-silyl carbocation. This pathway is again observed only for methanol, where it accounts for the formation of **12**, while with phenol, the corresponding product is not found. The third pathway **c** involves a rearrangement and leads to two analogous compounds, **9** (with phenol) and **13** (with methanol), and to the compound **10**.

Scheme 7

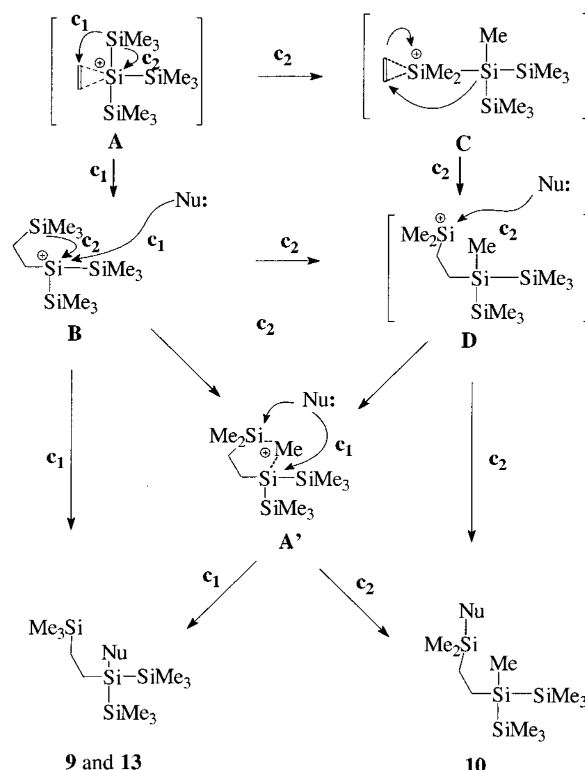

Pathway **c** appears to be complicated, and several possible mechanisms can be proposed to rationalize the formation of the observed products (**c_1** and **c_2**, Scheme 7). The original bridged siliconium cation **A** could undergo a 1,2-shift of one of the trimethylsilyl substituents to the bridging carbon (**c_1**), resulting in an open-chain bis(trimethylsilyl) substituted silyl cation **B** or a cyclic structure **A′** with a bridging methyl. A 1,2-shift is in line with the reported computational result that the bridged β-silylethyl cation is higher in energy than the ethylsilylium ion, $H_2Si^+-CH_2-CH_3$.[22] Similar 1,2-shifts of a trimethylsilyl group in α-tris(trimethylsilyl)silyl carbocations from silicon to carbon were reported earlier.[23] The open-chain bis(trimethylsilyl) substituted silyl cation **B** can then either be attacked by a nucleophile to produce the corresponding products **9** or **13** (**c_1**) or further rearrange via a methide abstraction by the positively charged silicon from the trimethylsilyl group attached to a carbon atom, resulting in a new open-chain dimethyl substituted silyl cation **D** (**c_2**). Cation **A** could also undergo a methide abstraction by the siliconium cation from one of the trimethylsilyl substituents resulting in a new bridged cation **C** (**c_2**), which could rearrange to **D** via a 1,3-shift. When attacked by a nucleophile, the open-chain dimethyl substituted silyl cation **D** would provide the rearranged compound **10** (**c_2**).

Another way of explaining the formation of compounds **9**, **13**, and **10** is by postulating that the open-chain cations **B** and **D** actually exist as the cyclic silyl

(12) Steinberger, H.-U.; Müller, T.; Auner, N.; Maeker, C.; Schleyer, P. v. R. *Angew. Chem., Int. Ed. Engl.* **1997**, *36*, 626.
(13) Wierschke, C.; Chandrasekhar, J.; Jorgensen, W. J. *J. Am. Chem. Soc.* **1985**, *107*, 1496.
(14) Ibrahim, M. R.; Jorgensen, W. J. *J. Am. Chem. Soc.* **1989**, *111*, 819.
(15) Drewello, T.; Burgers, P. C.; Zummack, W.; Apeloig, Y.; Schwarz, H. *Organometallics* **1990**, *9*, 989 and references therein.
(16) Mishima, M.; Kang, C. H.; Fujio, M.; Tsuno, Y. *Chem. Lett.* **1992**, 2439.
(17) Hudrlik, P. F.; Peterson, D. *J. Am. Chem. Soc.* **1975**, *97*, 1464.
(18) Jarvie, A. W.; Holt, A.; Thompson, J. *J. Chem. Soc. B* **1970**, 746.
(19) Cook, M. A.; Eaborn, C.; Walton, D. R. M. *J. Organomet. Chem.* **1970**, *24*, 301.
(20) Shimizu, N.; Hayakawa, F.; Watanabe, S.; Tsuno, Y. *Bull. Chem. Soc. Jpn.* **1993**, *66*, 153.
(21) Dickhaut, J.; Giese, B. *Org. Synth.* **1992**, *70*, 164.
(22) Ketvirtis, A. E.; Bohme, D. K.; Hopkinson, A. C. *Organometallics* **1995**, *14*, 347.
(23) Sternberg, K.; Oehme, H. *Eur. J. Inorg. Chem.* **1998**, 177.

Table 1. Product Ratios[a] from the Acidolysis of 4

path	Nu: MeOH (%)	PhOH (%)
a	12 (17)	0 (13)
b	48	0
$\mathbf{c_1}$	30	71
$\mathbf{c_2}$	0	10

[a] The results in parentheses include the yield of $(Me_3Si)_3SiH$.

cation **A′** bridged by a methyl group. Cation **A′** could be attacked by the nucleophile at either one of the two positively charged silicon atoms, resulting either in **9** and **13** or in **10**. The formation and properties of a related H^+-bridged silyl cation were described recently.[24]

Product ratios (Table 1) shed some light on the relative rates of the processes **a**, **b**, and **c** described above. The differences between the results in methanol and in phenol are readily rationalized by the proposed mechanism. In the case of acidolysis in methanol, product **12** resulting from the process **b** is the most abundant, followed by product **13** from the process $\mathbf{c_1}$ and finally by product **11** from the process **a**. Acidolysis in phenol leads predominantly to product **9** resulting from the process $\mathbf{c_1}$ and to a small amount of product **10** resulting from the process $\mathbf{c_2}$. It appears that the attack on the positively charged silicon atom of the bridged cation **A** is quite sterically hindered, such that only the small nucleophile methanol can attack, and even for methanol the rate of the addition is slow. Addition to the bridging carbon atom of **A** appears to be the fastest in methanol. In phenol, it is much slower, probably due to its lower nucleophilicity rather than steric hindrance, which in this case, should not be very important. The slow rate of addition of phenol provides the bridged cation **A** with enough time to rearrange, and it predominantly forms product **9** via the pathway $\mathbf{c_1}$. The rearrangement $\mathbf{c_1}$ must be quite fast, since even in methanol, **13** accounts for a substantial part of the reaction products. The second rearrangement $\mathbf{c_2}$ does not compete well, since its product **10** is observed only in phenol and only in a small amount. Finally, it appears that the product **10** is formed via the intermediate **A′** rather than **D** (Scheme 7); attack $\mathbf{c_2}$ in **D** is less sterically hindered than in **A′**, and **D** would be expected to predominantly lead to **10**.

By analogy, one would expect similar mechanisms for the acidolysis reaction of the copolymers **6** and **7**. The first step probably involves a fast proton transfer equilibrium between the photogenerated acid and the ester group. Step two is the slow, rate-determining cleavage to generate free carboxylic acid and a β-silyl carbocation. The fate of the liberated cation depends on the nature of the R group. Nucleophilic attack by phenol or water at silicon occurs in the case of R = Me. In the case of bulky silyl substituents, R = $SiMe_3$, fragmentation and rearrangements take place and the resulting species react with hydroxyl sources (such as phenols and/or water). In both cases, the protons necessary for chemical amplification to occur are regenerated.

An analysis of the ^{29}Si and ^{13}C NMR spectra of processed polymer films provides data on the fate of the 2-[tris(trimethylsilyl)silyl]ethyl moiety upon exposure

(24) Müller, T. *Angew. Chem. Int. Ed.* **2001**, *40*, 3033.

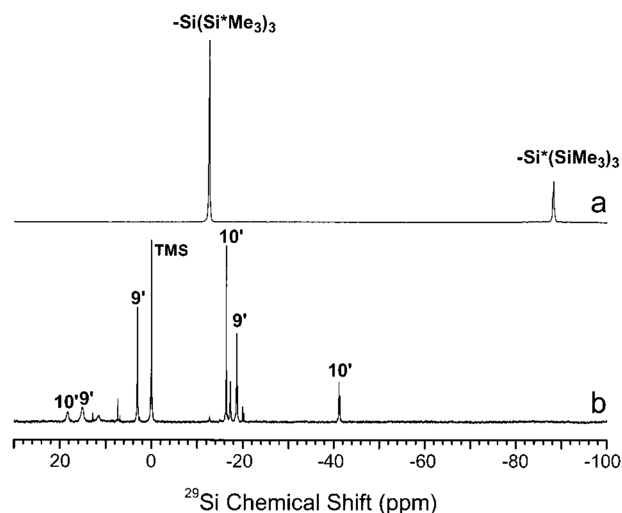

Figure 5. ^{29}Si NMR spectra of **7** before (a) and after (b) photolithography.

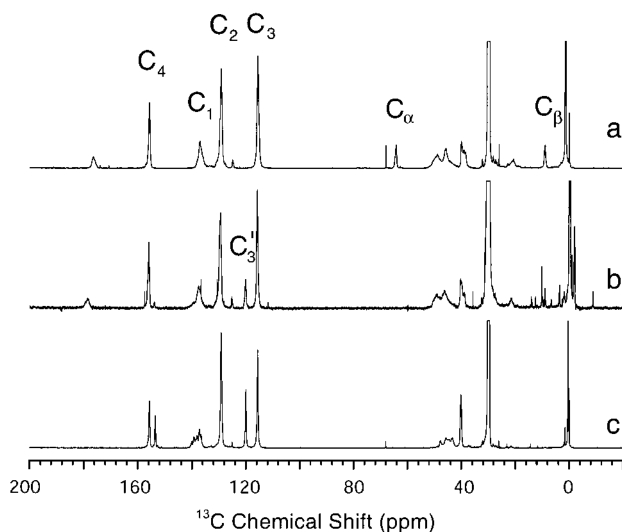

Figure 6. ^{13}C NMR spectra of **7** before (a) and after (b) photolithography, and ^{13}C NMR spectrum of partially trimethylsilylated polyhydroxystyrene **14** (c).

and baking of the resist film. The spectra shown in Figures 5 and 6 show complete cleavage of the reactive ester and formation of new products that remain in the film after postexposure bake. The resonance lines in the ^{29}Si spectrum of Figure 5b are labeled according to their assignments to structures analogous to the model compounds **9** and **10**, where the hydroxystyrene monomer unit plays the role of phenol. The resonances from the ^{29}Si nucleus that is closest to the polymer attachment point appear broad, most likely due to heterogeneity of the polymer microstructure. The ^{13}C NMR spectrum of Figure 6b shows that a significant fraction of the hydroxystyrene units undergoes silylation. The chemical shift of the aromatic C(3) resonance at 116 ppm is a particularly sensitive indicator, as there is a 4 ppm downfield shift upon silylation. The assignment of this new resonance C(3)′ is consistent with the spectrum of an authentic sample of partially trimethylsilylated polyhydroxystyrene **14** (Figure 6c). Integration of the C(3)′ resonance of Figure 6b relative to the entire aromatic region gives an estimate of 18% for the degree of silylation of hydroxystyrene monomer units. Other resonance lines of note in the ^{13}C NMR spectrum of the

resist film are the silicon-attached methylene carbon resonances in the range of 3−15 ppm and the peak at −9 ppm which is due to a silyl triflate species.

Conclusions

We have described a positive tone 248 nm bilayer resist system based on new high silicon content monomers, 2-(trimethylsilyl)ethyl methacrylate (**1**) and 2-[tris(trimethylsilyl)silyl]ethyl methacrylate (**2**). These monomers are acid labile, with a reactivity comparable to the *t*-butyl ester of poly(methacrylic acid). Their imageable 4-hydroxystyrene based copolymers containing up to 15 wt % silicon (in the case of **7**) are readily prepared. Line space arrays with features down to 140 nm have been printed by using copolymer **7**. These copolymers have etch selectivities of approximately 20:1 at silicon contents of 10−12 wt %, comparable to the selectivities of silicon systems based on unreactive structures.

We have studied model compounds to understand the processes that occur upon irradiation of the resists based on **1** and **2**. Acid-catalyzed cleavage of the model **3**, 2-(trimethylsilyl)ethyl acetate, is proposed to proceed via a nucleophilic attack on the silicon atom of the protonated acetate. Protonation of 2-[tris(trimethylsilyl)-silyl]ethyl acetate (**4**) in methanol or phenol gives results compatible with the intermediacy of a bridged siliconium cation, which reacts with nucleophiles along three pathways, with the phenol nucleophile attacking a silicon atom. This explains why under the actual photolithographic conditions, silylation of the phenolic hydroxyl groups is significant for the copolymer **7**.

Experimental Section

General. Freshly distilled solvents and reagents were used after being dried as follows: methanol with magnesium methoxide; chloroform with CaH_2; phenol with benzene/CaH_2; triflic acid with triflic anhydride. *t*-Butyl acetate was purchased from Aldrich and used without further purification. NMR measurements for the model compounds were done with a Varian XRS-300 spectrometer operating at 299.96, 75.43, and 59.59 MHz for ^{1}H, ^{13}C, and ^{29}Si nuclei, respectively. Chemical shift values are relative to TMS for all nuclei and are given in δ ppm. Elemental analyses were performed by Desert Analytics. GC/MS analyses were done on a HP-5988A system. NMR measurements for the photoresist materials were done with a Bruker AM-500 spectrometer operating at 500.14, 125.77, and 99.36 MHz for ^{1}H, ^{13}C, and ^{29}Si, respectively. The ^{13}C and ^{29}Si spectra were obtained by using inverse-gated ^{1}H decoupling to minimize NOE effects. Chromium(III) acetylacetonate, Cr(acac)$_3$, was used to shorten the T_1 relaxation times. The polymer samples were prepared by irradiating 1 μm thick films of the copolymer **7** (80:20 monomer ratio) containing di-*t*-butyliodonium triflate (5 wt %). After the exposure (254 nm), the coated 5″ silicon wafers were baked at 130 °C for 60 s and the polymer was scraped off. This polymer (42 mg) was mixed with Cr(acac)$_3$ (21 mg) in acetone-d_6 (500 mg). The poly(hydroxystyrene-trimethylsilyloxystyrene) sample was prepared by dissolving the polymer (212 mg) and Cr(acac)$_3$ (21 mg) in acetone-d_6 (500 mg).

Separation Techniques. All mixtures were analyzed by using a Varian 3400 analytical GC instrument with a 0.2 mm × 25 m 0.33 μm RSL-150 5% cross-linked silica capillary column. All separations were performed by using a Varian 3400 preparative GC with a 1/4″ × 21′ 5% OV-7 80/100 Chromosorb GHP packed column. Individual compounds were purified to better than 99.5% purity (as determined by analytical GC).

2-(Trimethylsilyl)ethyl Methacrylate (1). Methacryloyl chloride (11.50 g, 0.11 mol) in dichloromethane (50 mL) was added dropwise into a solution of 2-(trimethylsilyl)ethanol (Aldrich, 12.00 g, 0.10 mol), pyridine (8.7 g, 0.11 mol), and phenothiazine (25 mg) in dichloromethane (150 mL) at room temperature, and the mixture was stirred for 2 h. The solids were filtered off, and the solution was washed with 5% HCl followed by deionized water and then brine. It was dried over anhydrous $MgSO_4$ and was concentrated in vacuo. Fractional distillation at 85 °C and 0.5 mmHg gave **1** (10 g, 53.5% yield). ^{1}H NMR (CDCl$_3$): δ 6.03 (1H, m, vinyl), 5.48 (1H, m, vinyl), 4.11 (2H, t, OCH$_2$), 2.00 (3H, m, CH$_3$), 0.94 (2H, t, SiCH$_2$), 0.01 (9H, s, SiMe$_3$). ^{13}C NMR (CDCl$_3$): δ 167.5 (C=O), 136.7 (=C<), 124.8 (=CH$_2$), 62.7 (OCH$_2$), 18.2 (CH$_3$), 17.2 (SiCH$_2$), −1.6 (SiCH$_3$). IR (neat): 2955, 2892, 1722, 1644, 1456, 1047, 1325, 1296, 1248, 1165, 1044, 933, 841 cm^{-1}. MS/EI *m*/*e* (relative intensity): 185 (4), 171 (17), 158(1), 143 (100), 130 (3), 116 (4), 107 (1), 99 (14), 85 (4), 73 (50), 59 (4), 51 (1). Anal. Calcd: C, 58.01; H, 9.74. Found: C, 57.93; H, 9.92.

2-[Tris(trimethylsilyl)silyl]ethyl Methacrylate (2). To a 500 mL, three-necked round-bottomed flask equipped with an ice bath, magnetic stirbar, a thermo-well, and a constant-pressure addition funnel with a nitrogen inlet was added 2-[tris(trimethylsilyl)silyl]ethanol (18.7 g, 64 mmol), triethylamine (7.43 g, 75 mmol), and methylene chloride (125 mL). The addition funnel was charged with freshly distilled methacryloyl chloride (7.6 g, 75 mmol). The flask was cooled to 5 °C under nitrogen, and the methacryloyl chloride was added at a rate such that the temperature remained below 10 °C. The stirred reaction mixture was allowed to warm to room temperature overnight. Water (~150 mL) was added, and the stirring was continued for an additional 15 min. The mixture was allowed to settle; the top layer was separated and washed sequentially with water (2 × 150 mL) and brine (200 mL). The methylene chloride solution was dried over $MgSO_4$, filtered, and evaporated on a rotary evaporator. The resulting light yellow oil was taken up in hexane (150 mL) and filtered through silica gel (50 g). The silica gel was washed with hexane (200 mL), and the combined organic solution was evaporated on a rotary evaporator. The residual solvent was driven off with a stream of dry air, and 4-methoxyphenol (MeHQ) was added to approximately 200 ppm. The yield of **2** was 17.8 g (78%) of a clear, colorless liquid. Note: This material can be distilled (bp 125 °C at 1 mmHg) with significant loss due to polymerization. ^{1}H NMR (C$_6$D$_6$): δ 5.90 (1H, s, vinyl), 5.35 (1H, s, vinyl), 4.01 (2H, m, CH$_2$), 1.75 (3H, s, CH$_3$), 1.07 (2H, m, CH$_2$), 0.03 (27H, s, [SiMe$_3$]$_3$). ^{13}C NMR (CDCl$_3$): δ 8.82 (CH$_2$-Si), 18.29 (CH$_3$), 65.0 (OCH$_2$), 124.8 (=CH$_2$), 136.8 (=C), 167.3 (O=C). IR (neat): 2948, 2890, 1716, 1308, 1287, 1245, 1158, 831, 686, 616 cm^{-1}. ^{29}Si NMR (CDCl$_3$): δ −12.6 (TMS), −87.6 (CH$_2$Si−). MS/EI (relative intensity) 360 (M$^+$, 0.1), 345 (2), 332 (2), 317 (4), 287 (3), 259 (100), 201 (28), 187 (2), 174 (4), 159 (3), 145 (3), 131(4), 117 (4), 99 (2), 73 (30), 69 (45). Anal. Calcd: C, 49.93; H, 10.06. Found: C, 49.94; H, 10.17.

2-(Trimethylsilyl)ethyl Acetate (3)[25] and 2-[Tris(trimethylsilyl)silyl]ethyl Acetate (4).[26] These were prepared according to the literature procedures.

3-[Tris(trimethylsilyl)silyl]propyl Acetate (5). To a 2 L four-necked round-bottomed flask equipped with an addition funnel, condenser, thermocouple temperature gauge, magnetic stirrer, heating mantle, and argon inlet was added allyl acetate (8.0 g, 80 mmol), AIBN (3.14 g, 19.2 mmol), and toluene (800 mL). The addition funnel was charged with tris(trimethylsilyl)-silane (Aldrich, 23.8 g, 96 mmol). The flask was heated, and the silane was added dropwise over 10 min with vigorous stirring. The heating was continued at 92 °C for 5 h; the mixture was evaporated on a rotary evaporator, and the resulting yellow oil was distilled at 112 °C (1 mmHg) to yield 23.8 g (85%) of **5** as a clear, colorless oil. ^{1}H NMR (C$_6$D$_6$): δ 3.94 (2H, t, OCH$_2$), 1.69 (3H, s, CH$_3$), 0.75 (4H, m, 2 CH$_2$),

(25) Schraml, J.; Chvalovský, V.; Magi, M.; Lippmaa, E. *Collect. Czech. Chem. Commun.* **1978**, *43*, 3, 3365.
(26) Kopping, B.; Chatgilialoglu, C.; Zehnder, M.; Giese, B. *J. Org. Chem.* **1992**, *57*, 3994.

0.17 (27H, s, $SiMe_3$). $^{13}C\{^1H\}$ NMR (C_6D_6): δ 170.75 (C=O), 67.8 (OCH_3), 29.36, 21.30, 4.52 ($3CH_2$), 2.05 ($SiCH_3$). $^{29}Si\{^1H\}$ NMR (C_6D_6): δ −13.59 ($SiMe_3$), −81.93 (Si). IR (neat): 2949, 2893, 1745, 1438, 1363, 1384, 1245, 1049, 835, 746, 687, 623 cm^{-1}. MS/EI *m*/*e* (relative intensity): 278 (1), 263 (10), 247 (1), 205 (5), 189 (4), 175 (10), 159 (5), 147 (3), 131 (8), 117 (5), 101 (2), 89 (2), 73 (100). Anal. Calcd: C, 43.10; H, 10.85. Found: C, 42.93; H, 11.01.

Poly{4-hydroxystyrene-*co*-[2-(trimethylsilyl)ethyl methacrylate]} (6). 4-Hydroxystyrene[27] (33.60 g of 25% THF solution, 0.070 mole), **1** (5.61 g, 0.03 mol), and 2-propanol (17 g) were placed in a round-bottomed flask equipped with a condenser and a nitrogen inlet. AIBN (0.66 g, 4 mol %) was added, and it was stirred until it dissolved. The solution was evacuated with the aid of a Firestone valve and purged with nitrogen. This was repeated three more times, and the contents were then heated to reflux for 18 h. The solution was diluted with 2-propanol (50 mL) and added dropwise into deionized water (1.0 L). The precipitated polymer was filtered (frit), washed twice with water (100 mL), and dried under vacuum at 60 °C. Yield: 12.38 g (31.6%). $M_n = 6700$, $M_w/M_n = 1.92$, $T_g = 120$ °C. ^1H NMR (acetone-d_6): δ 7.96 (broad, OH), 6.72 (broad, OPh), 0.0 (broad, $SiCH_3$). ^{13}C NMR (acetone-d_6): δ 176.7 (C=O), 156.2, 138.7, 129.9, 115.9 (OPh), 62.6 (OCH_2), 18.0 ($SiCH_2$), −1.1 ($SiCH_3$). IR (neat): 3385, 3023, 2945, 1722, 1697, 1615, 1591, 1514, 1441, 1369, 1252, 1214, 1170, 1049, 933, 832 cm^{-1}.

Poly(4-hydroxystyrene-*co*-{2-[tris(trimethylsilyl)silyl]-ethyl methacrylate}) (7). 4-Hydroxystyrene[27] (19.20 g as 25% THF solution, 0.040 mol), **2** (3.80 g, 0.010 mol), and THF (11.40 g) were placed in a round-bottomed flask equipped with a condenser and a nitrogen inlet. AIBN (0.33 g, 4 mol %) was added and stirred until it was dissolved. The solution was evacuated with the aid of a Firestone valve and purged with nitrogen. This was repeated three more times. The contents were then heated to reflux for 18 h. The solution was diluted with acetone (50 mL) and added dropwise into hexanes (1.0 L). The precipitated polymer was filtered (frit), washed twice with hexanes (100 mL), and dried under vacuum at 60 °C. Yield: 5.4 g (23.5%). $M_n = 5800$, $M_w/M_n = 1.70$, $T_g = 163$ °C. ^1H NMR (acetone-d_6): δ 7.73 (broad, OH), 6.45 (broad, OPh), 0.0 (broad, $SiCH_3$), and other broad peaks. ^{13}C NMR (acetone-d_6): δ 177.0 (C=O), 156.1, 137.6, 129.6, 128.4 (OPh), 69.6 (OCH_2), 9.3 ($SiCH_3$), 1.6 ($SiCH_3$). Composition as determined by inverse gated ^{13}C NMR: 76:24. IR (neat): 3411, 2946, 1699, 1613, 1513, 1445, 1373, 1245, 1171, 838 cm^{-1}.

Acidolysis of 3. Dry triflic acid (8.8 μL, 0.1 mmol) was added under an atmosphere of Ar to a degassed solution of **3** (0.8 g, 5 mmol) in dry phenol (1.88 g, 20 mmol). The reaction mixture was stirred for 12 h at room temperature; dry pyridine (0.474 g, 6 mmol) was added, followed by dry hexane (20 mL). The precipitated pyridinium salts were filtered off, and the resulting solution was analyzed by analytical GC and used for separations by preparative GC.

Acidolysis of 4. The acidolysis of **4** (1.67 g, 5 mmol) with dry triflic acid (8.8 μL, 0.1 mmol) was conducted in full analogy to the acidolysis of **3**.

Bis(trimethylsilyl)[2-(trimethylsilyl)ethyl]phenoxysilane (9). ^1H NMR (C_6D_6): δ 7.08 (2H, m, *o*-Ph), 6.96 (2H, m, *m*-Ph), 6.81 (1H, m, *p*-Ph), 1.14−0.79 (4H, AA′BB′, 2 CH_2), 0.20 (18H, s, 2 $SiMe_3$), 0.03 (9 H, s, $SiMe_3$). $^{13}C\{^1H\}$ NMR (C_6D_6): δ 158.15, 129.71, 121.53, 120.05 (OPh), 10.05 (CH_2), 8.68 (CH_2), −0.54 (2 $SiMe_3$), −2.19 ($SiMe_3$). $^{29}Si\{^1H\}$ NMR (C_6D_6): δ 15.04 ($SiMe_3$), 3.14 (Si), −18.52 (2 $SiMe_3$). IR (neat): 3026, 2923, 2895, 1927, 1595, 1491, 1398, 1248, 1130, 1049, 1022, 858, 837, 760, 690 cm^{-1}. MS/EI: *m*/*e* (relative intensity) 353 (1), 295 (3), 267 (2), 253 (1), 237 (3), 207 (3), 193 (5), 174 (5), 159 (3), 145 (5), 135 (10), 117 (2), 85 (1), 73 (100). Anal. Calcd: C, 53.36; H, 9.84. Found: C, 53.52; H, 10.05.

(27) Hirao, A.; Yamaguchi, K.; Takenaka, K.; Suzuki, K.; Nakahama, S. *Macromol. Rapid Commun.* **982**, *3*, 941.

Bis(trimethylsilyl)[2-(dimethylphenoxysilyl)ethyl]-methylsilane (10). ^1H NMR (C_6D_6): δ 7.10 (2H, m, *o*-Ph), 6.93 (2H, m, *m*-Ph), 6.84 (1H, m, *p*-Ph), 10.84 (4H, bs, 2 CH_2), 0.21 (6H, s, $SiMe_2$), 0.15 (18H, s, 2 $SiMe_3$), 0.13 (3H, s, CH_3). $^{13}C\{^1H\}$ NMR (C_6D_6): δ 155.92, 129.83, 121.76, 120.31 (OPh), 12.32 (CH_2), 3.29 (CH_2), −0.69 (2 $SiMe_3$), −1.96 ($SiMe_2$), −9.01 (CH_3). $^{29}Si\{^1H\}$ NMR (C_6D_6): δ 18.52 ($SiMe_2$), −16.29 ($SiMe_3$), −40.78 (Si). IR (neat): 3039, 2951, 2893, 1927, 1597, 1493, 1404, 1252, 1164, 1132, 1053, 916, 853, 779, 690 cm^{-1}. MS/EI: *m*/*e* (relative intensity) 353 (0.1), 295 (5), 267 (1), 237 (2), 209 (1), 193 (2), 151 (5), 131 (2), 117 (2), 85 (1), 73 (100). Anal. Calcd: C, 53.36; H, 9.84. Found: C, 53.32; H, 9.91.

Tris(trimethylsilyl)methoxysilane (11).[28] ^1H NMR (C_6D_6): δ 3.29 (3H, s, OCH_3), 0.25 (27H, s, $SiMe_3$). $^{13}C\{^1H\}$ NMR (C_6D_6): δ 55.63 (OCH_3), 0.47 ($SiCH_3$). $^{29}Si\{^1H\}$ NMR (C_6D_6): δ 4.43 (Si), −15.77 ($SiMe_3$).

Bis(trimethylsilyl)[2-(trimethylsilyl)ethyl]methoxysilane (12). ^1H NMR (C_6D_6): δ 3.44 (3H, t, CH_2), 3.13 (3H, s, OCH_3), 1.25 (3H, t, CH_2), 0.22 (27H, s, $SiMe_3$). $^{13}C\{^1H\}$ NMR (C_6D_6): δ 72.43 (CH_2), 57.71 (OCH_3), 9.66 (CH_2), 1.23 ($SiCH_3$). $^{29}Si\{^1H\}$ NMR (C_6D_6): δ −12.40 ($SiMe_3$), −85.75 (Si). IR (neat): 2953, 2897, 2823, 1400, 1246, 1080, 856, 836, 733, 710, 690 cm^{-1}. MS/EI: *m*/*e* (relative intensity) 306 (0.1), 291 (1), 263 (1), 233 (3), 217 (1), 205 (3), 191 (2), 175 (15), 147 (5), 131 (10), 117 (3), 101 (2), 89 (3), 73 (100). Anal. Calcd: C, 46.99; H, 11.17. Found: C, 46.76; H, 11.28.

Tris(trimethylsilyl)(2-methoxyethyl)silane (13).[29] ^1H NMR (C_6D_6): δ 3.36 (3H, s, OCH_3), 0.97−0.71 (4H, AA′BB′, 2 CH_2), 0.23 (18H, s, $2SiMe_3$), 0.04 (9H, s, $SiMe_3$). $^{13}C\{^1H\}$ NMR (C_6D_6): δ 53.22 (OCH_3), 10.02 (CH_2), 7.14 (CH_2), −0.38 (2 $SiMe_3$), −2.18 ($SiMe_3$). $^{29}Si\{^1H\}$ NMR (C_6D_6): δ 14.89 ($SiMe_3$), 3.02 (Si), −19.68 ($2SiMe_3$).

Poly(4-hydroxystyrene-*co*-4-trimethylsilyloxystyrene) (14). Poly(4-hydroxystyrene) (Hoechst Celanese, M_w ∼10 000) (6 g, 0.05 mol of monomer units) was dissolved in dry THF (50 mL). Hexamethyldisilazane (4.0 g, 0.025 mol) was added; the mixture was heated to reflux under nitrogen for 90 min and was added dropwise into hexanes (500 mL). The precipitated polymer was filtered (glass frit funnel), washed twice with 50 mL of hexanes, and dried under vacuum at 60 °C for 48 h. NMR analysis indicated ∼38% silylation (copolymer ratio, 62:38). ^1H NMR (acetone-d_6): δ 7.70 (broad, OH), 6.40 (broad, OPh), 0.0 (broad, $SiCH_3$). ^{13}C NMR (acetone-d_6): δ 155.7, 153.6, 138.0, 129.2, 120, 115.7, 45.7, 40.2, 0.3. IR (neat): 3385, 3027, 2960, 2921, 2844, 1610, 1509, 1441,1364, 1252, 1170, 1102, 1054, 919, 841, 754 cm^{-1}.

Kinetic Measurements. Equimolar amounts of *t*-butyl acetate (0.023 g, 0.2 mmol, Aldrich, used without further purification) and **4** (0.035 g, 0.2 mmol) were placed in an NMR tube with a 60:40 mixture of methanol-d_4 (Aldrich, used without further purification) and chloroform-d_1 (dried over CaH_2, freshly distilled), and 1 μL (0.01 mmol) of freshly distilled anhydrous HOTf was added to the solution. The mixture was stirred at 25 °C, and the relative concentrations of the starting materials were measured by recording ^1H NMR spectra of the mixture with nitromethane as an internal standard and integrating the appropriate signals. Eight points were recorded over a period of 12 h. The results were plotted as ln(*S*) vs time, where *S* is an area of the peak at 1.66 ppm for *t*-butyl acetate (*t*-Bu−O) and at 4.40 ppm for **4** (CH_2−O). First-order rate constants obtained in this way were 1.4×10^{-5} s^{-1} for *t*-butyl acetate and 2.9×10^{-5} s^{-1} for **4**.

Acknowledgment. This work was supported by IBM, Inc., and NSF (CHE-9819179).

CM010660I

(28) Lei, D.; Chen, Y.-S.; Boo, B. H.; Frueh, J.; Svoboda, D. L.; Gaspar, P. P. *Organometallics* **1992**, *11*, 559.
(29) Zhang, S.; Ezhova, M. B.; Conlin, R. T. *Organometallics* **1995**, *14*, 1471.